Applied Clay Science 134 (2016) 246–256

Contents lists available at ScienceDirect

Applied Clay Science

journal homepage: www.elsevier.com/locate/clay

Research paper

Very low-grade secondary minerals as indicators of palaeo-hydrothermal systems in the Upper Cretaceous volcanic succession of Hannah Point, Livingston Island, Antarctica

Joaquin Bastias [a,b,*], Francisco Fuentes [c], Luis Aguirre [a], Francisco Hervé [a,c], Alain Demant [d], Katja Deckart [a], Teresa Torres [e]

[a] Universidad de Chile, Departamento de Geología, Plaza Ercilla 803, Santiago, Chile
[b] University of Geneva, Department of Earth Sciences, rue de Mairaîchers 13, Geneva, Switzerland
[c] Universidad Andres Bello, Facultad de Ingenieria, Salvador Sanfuentes 2357, Santiago, Chile
[d] Laboratoire de Pétrologie Magmatique, Université Aix Marseille III, 13397 Marseille Cedex 20, France
[e] Universidad de Chile, Departamento de Producción Agrícola, Santiago, Chile (Correo 1004)

ARTICLE INFO

Article history:
Received 21 January 2016
Received in revised form 22 July 2016
Accepted 26 July 2016
Available online 30 July 2016

Keywords:
Zeolite
Low-temperature metamorphism
Smectite-chlorite
Geothermal
Burial metamorphism
Antarctica
Hydrothermal alteration

ABSTRACT

The Upper Cretaceous basic volcanic succession in Hannah Point, Livingston Island, Antarctica, presents a widespread occurrence of very low-grade secondary minerals. They occur filling amygdules, veins and veinlets, and replacing phenocrysts and groundmass/matrix. The paragenetic associations include minerals such as laumontite, heulandite, stilbite and clinoptilolite; mafic phyllosilicates corresponding to chlorite and smectite mixed layers (compositions ranging from 57% to 84% of chlorite), albite, calcite and minor celadonite. The mineral assemblages indicate, based on laboratory and field studies, these mineral paragenesis temperatures of 150–200 °C and pressures of 600–1.800 bars, which agrees with the calculated equilibrium temperatures of 160–190 °C, using chlorite geothermometry. These burial pressures, which were estimated from paragenesis, cannot be attained considering the present thickness of 500 m of the sequence, because at least 1 km of erosion is required to produce the mineral associations. Based on textural evidence, three successive stages are proposed to explain the genesis of the secondary minerals: (1) mafic phyllosilicates ± celadonite, (2) zeolites and (3) calcite. The characteristics of these stages point to a regional burial metamorphism (stage 1) superimposed by hydrothermal alteration (stages 2 and 3). The mineral paragenetical evolution can be used as a proxy for the prospection of modern geothermal reservoirs by allowing the identification of hydrothermal alteration processes and burial metamorphism.

1. Introduction

Very low-grade secondary minerals in basic volcanic rocks are excellent indicators of the different pressure and temperature conditions during the upper crust evolution mainly in oceanic provinces and continental flood basalts (e.g. Robinson and Bevins, 1999). The presence of these minerals is also useful in providing critical information for assessing geothermal gradients in continental arc settings (e.g., Fuentes et al., 2004; Miron et al., 2012). Temperature, pressure, bulk-rock composition, fluid compositions and porosity-permeability control the formation and compositional variations of the common very low-grade minerals in basic igneous rocks such as zeolites, mafic phyllosilicates, prehnite, pumpellyite and epidote (e.g., Alt, 1999). Understanding the mechanisms of generation of these minerals is not only useful to obtain information about physic-chemical conditions that affected the crust, but also for the prospection of geothermal energy.

The occurrence of thermal metamorphism and/or hydrothermal alteration was already reported during the early scientific expeditions to the South Shetland Islands (e.g. Araya and Hervé, 1965; Smellie, 1979). The first detailed study by Willan and Armstrong (2002) addresses the alteration assemblages on King George Island. Recently, they also have been documented in King George Island (Fuentes et al., 2015) and Livingston Island (Bastias et al., 2013).

The present study aims to complement our knowledge of thermal metamorphism and/or hydrothermal alteration on the archipelago of the South Shetland Island and focuses on the rock sequence at Hannah Point, Livingston Island. This island is the second largest island of the 550 km long South Shetland archipelago (Fig. 1). Hannah Point is a small outcrop area located on the south-central coast (Fig. 1). Secondary minerals filling amygdules in the basic volcanic rocks are exceptional and widespread features in the volcanic sequence of the island.

* Corresponding author at: Universidad de Chile, Departamento de Geología, Plaza Ercilla 803, Santiago, Chile.
E-mail address: j.bastias.silva@gmail.com (J. Bastias).

http://dx.doi.org/10.1016/j.clay.2016.07.025
0169-1317/

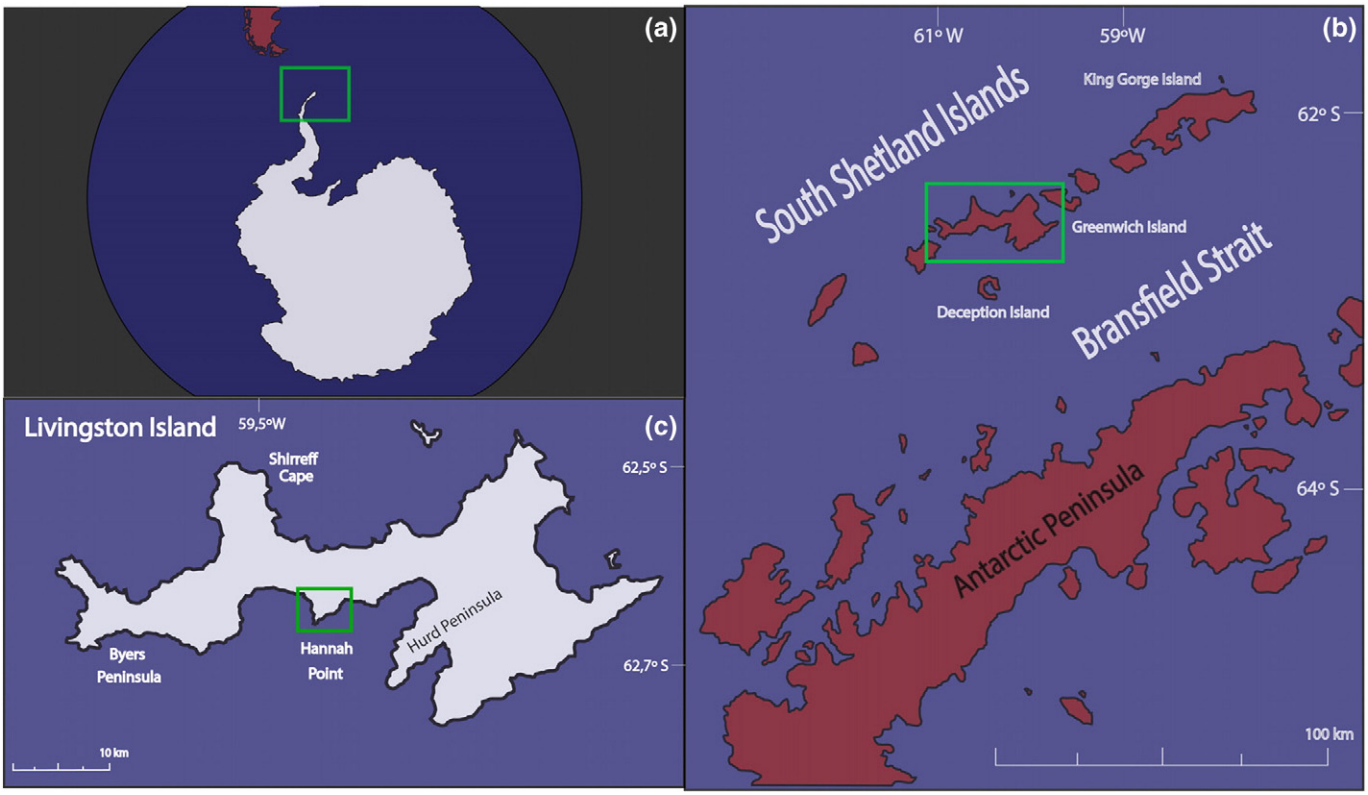

Fig. 1. General location of the study area. (a) Antarctic Peninsula in a global context; the study area is marked by a green square. (b) Antarctic Peninsula and the South Shetland Islands; in a green square Livingston Island. (c) Livingston Island, in a green square Hannah Point.

The tectonic and thermal evolution of the South Shetland Islands and the Antarctic Peninsula is the result of several processes typical of active subduction margins, in this case the subduction of the Phoenix Plate since the Early Mesozoic to the Cenozoic times (e.g. Hervé et al., 2005). Extensional processes occurring during the Cenozoic have led to the formation of the Bransfield Strait, a narrow extensional basin (65 km wide) that separates the South Shetland Islands from the Antarctic Peninsula (e.g. Barker, 1982; Solari et al., 2008).

The present paper aims to contribute to the characterization and determination of the mineral assemblages, mineral chemistry, and the pressure and temperature under which the very low-grade secondary mineral assemblages of Hannah Point were generated. This result will provide a better understanding of the processes that contributed to the formation of these mineral paragenesis formation, so widespread in the South Shetland Island arc, allowing to increase our knowledge and applications of these mineral indicators to very-low grade metamorphism.

2. Geological background

The South Shetland Island arc is the most conspicuous geological feature present in the archipelago. It was formed as a response to the subduction of the Pacific oceanic crust in a southeast direction under the continental crust of the Antarctic Peninsula (Ref.). Its volcanic activity record ranges between 135 and 47 Ma (Smellie et al., 1984; Haase et al., 2012), featuring a decreasing age trend from southwest to northeast (Pankhurst and Smellie, 1983; Smellie et al., 1984), which has been confirmed by recent geochronological studies (Haase et al., 2012). They mainly consist in lavas and associated volcaniclastic rocks (Smellie et al., 1984) of calk-alkaline to tholeitic affinities. These rocks do not show a clear systematic change with age or geographical location (Haase et al., 2012) suggesting that, despite the long lasted volcanic activity (more than 100 my), there is not a clear evolution from or towards a more enriched or evolved magma is observed.

The basement consists of Jurassic to Cretaceous turbidite sequences from the Cape Wallace Beds unit (Bastias and Hervé, 2013; Bastias, 2014), metamorphic rocks from the Scotia Metamorphic Complex (Grunow et al., 1992), and some minor acid intrusions on Livingston Island (Hervé et al., 2006) and Low Island (Bastias, 2014). In the case of the Antarctic Peninsula, the Mesozoic-Tertiary magmatic arc units were emplaced within the Triassic-Permian turbiditic rocks of the Trinity Peninsula Group (Leat et al., 1995), largely represented in the northern Antarctic Peninsula (e.g. Castillo et al., 2015), and in the archipelago of the Shetlands within the Jurassic-Cretaceous turbiditic sequences.

Hannah Point is part of the widespread occurrence of volcanic rocks from Livingston Island. With a thickness of c. 500 m of layered rocks, is probably the most extensive volcanic sequence of the archipelago. Pallàs et al. (1999) recognized five members within this succession, from base to top: (a) 120 m of polymictic volcaniclastic breccias, (b) 70 m of volcaniclastic breccias, (c) 65 m of basaltic lavas, (d) 65 m of volcaniclastic breccias, and (e) 150 m of andesitic lavas, suggesting that the rocks of this succession were emplaced as pyroclastic flows associated with explosive volcanic activity in a subaerial environment. The age has been determined by a combination of paleontology and geochronology. On the base of leaf imprints and fossil trunks Leppe et al. (2007) suggested a Late Cretaceous age. This was confirmed by Haase et al. (2012) based on $^{40}Ar/^{39}Ar$ whole rock data giving an age of 97.5 Ma.

2.1. Magmatic activity

Volcanic activity in the South Shetland Islands has been present active since the Late Cretaceous on Livingston Island (e.g. Smellie et al., 1984) and up to the Quaternary in Deception Island and other related offset arc volcanic islands (e.g. Barker, 1982). The Late Cretaceous

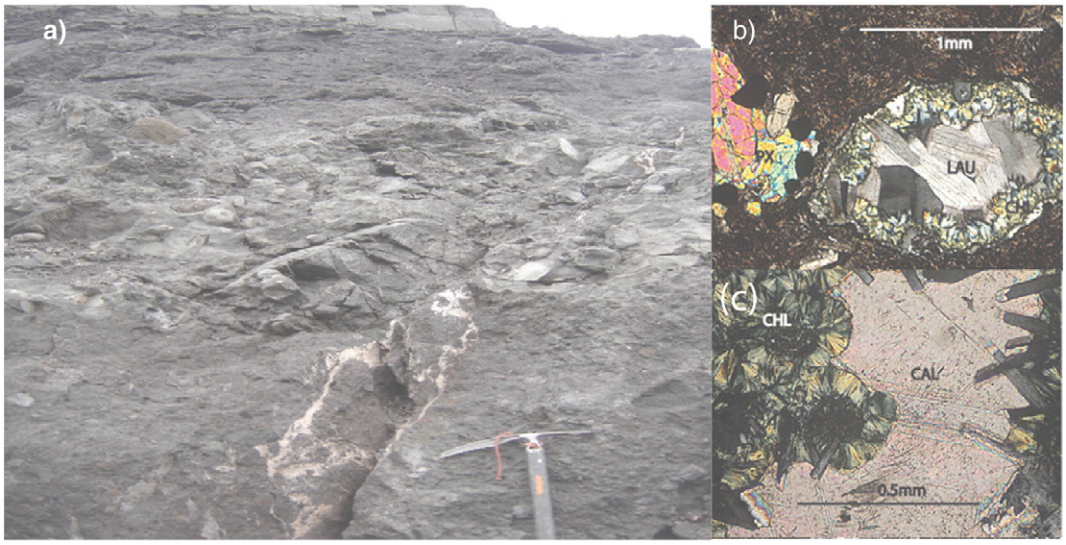

Fig. 2. Alteration styles at different scales in the volcanic succession of Punta Hannah. (a) Veins of secondary minerals cutting across the contact between the lava flows. (b) Amygdule with Chl-Sm mixed-layer (rim) and laumontite (core). (c) Former vesicle or amygdule filled with mafic phyllosilicates (Chl-Sm mixed-layer) then with prisms of laumontite and then with calcite. Abbreviations: LAU: laumontite, PX: pyroxene, CHL: Chl-Sm mixed-layer, CAL: calcite.

volcanic activity is well recorded on Livingston Island: in the western, Byers Peninsula, in the Start Hill Formation (Gracanin, 1983), in the northwest, Cape Shirreff (Smellie et al., 1996), in the northeast in Williams Point (Smellie et al., 1984) and at the south-center in Hannah Point (Leppe et al., 2007; Haase et al., 2012). The volcanic activity gradually gets younger further to the north of the archipelago, with the exception of King George Island where some Late Cretaceous rocks are present (e.g. Nawrocki et al., 2010).

The volcanic rocks, from the Upper Cretaceous through the Eocene, are cut by mafic dykes (Willan and Kelley, 1999). Few plutonic bodies of acidic compositions and Late Cretaceous and Eocene age have been recognized in the archipelago. They are mainly exposed in Livingston Island, Low Island and King George Island (Smellie et al., 1984; Hervé et al., 2006; Bastias, 2014).

3. Sampling and analytical procedures

Fieldwork in the volcanic succession of Hannah Point was carried out by a geological-paleontological Chilean expedition in February 2007 and completed in 2008 with emphasis on the volcanism.

Detailed petrographic studies of secondary mineral assemblages were conducted on a subset of representative samples in order to determine the mineral phases and their parageneses. The studies were carried out on macroscopic samples and thin sections using a standard polarized light microscope, and X-ray powder diffraction and electron-microprobe analysis of selected samples.

X-ray powder diffraction (XRPD) analysis of five samples was performed at the Laboratorio de Rayos X y Mineralogía of the Servicio Nacional de Geología y Minería (SERNAGEOMIN), Chile, using a Phillips diffractometer 1130/90 model with CuKα radiation operating at 40 kV, 20 mA, and divergence slit of 1°.

Chemical compositions of primary pyroxenes and plagioclases and of secondary mineral phases, mainly mafic phyllosilicates and zeolites, were determined on nine polished thin sections. Major and minor elements of the minerals were measured by wavelength-dispersive, electron probe microanalysis (EPMA) using a Cameca SX-100 electron microprobe fitted with five spectrometers of the "Service Commun Microsonde" (Université de Montpellier 2). The microprobe was operated at 20 kV accelerating potential and 10 nA beam current, with an electron beam of 5 μm in diameter and integrated counting times of 20–30 s. Synthetic and natural minerals were used as standards for calibration. Alkalis were determined first to minimize Na and K loss during measurements. A computer correction program (Merlet, 1994) was used to calculate the element concentrations. The accuracy of major element determinations is better than ±5% of the total values.

4. Mineralogy

At Hannah Point, the alteration of the volcanic rock is evident by the presence of veins, veinlets and amygdales (Fig. 2a). Phenocrysts and groundmass/matrix appear partially to totally replaced by low-temperature secondary minerals (Fig. 2b and c).

4.1. Primary mineralogy

The Late Cretaceous volcanic succession at Hannah Point is mostly composed of andesitic to basaltic pyroclastic rocks and lava flows. These rocks have been strongly altered, displaying a devitrified matrix/groundmass and a large percentage of secondary minerals within it. The primary minerals are olivine, plagioclase and pyroxene. Representative compositions of pyroxenes are presented in Table 1. They correspond to augite with an average composition of $Wo_{40}En_{43}Fs_{17}$ frequently altered to mafic phyllosilicates at their edges or along fractures. The primary plagioclases have andesine ($An_{55}Ab_{45}$) to anorthite ($An_{91}Ab_{09}$) composition (Fig. 3; Table 2).

4.2. Secondary mineralogy

4.2.1. Plagioclase alteration

Plagioclase phenocrysts, originally of andesine-anorthite compositions, have been strongly albitized to compositions between $An_{02}Ab_{98}$ and $An_{28}Ab_{72}$ (Fig. 3; Table 2). In addition to albite, these phenocrysts have been replaced extensively by zeolites, mafic phyllosilicates and calcite. The replacement can be partial, affecting the crystal edges and fractures, or total.

4.2.2. Mafic phyllosilicates

Mafic phyllosilicates are present as patches in primary plagioclases and pyroxenes, as partial or total replacement of primary plagioclase, pyroxene phenocrysts, groundmass/matrix, and filling veinlets and vesicles (Fig. 2). Celadonite is present in a few samples as partial alteration of clinopyroxene and olivine.

Representative microprobe analyses of mafic phyllosilicates, recalculated on the basis of a chlorite formula with 28 oxygens, are

Table 1
Representative microprobe analyses of pyroxenes from Late Cretaceous volcanic rocks at Hannah Point.

Analyzes	F12	F12	ARC	ARC
Point	49	50	56	51
SiO_2	50.56	50.28	51.75	51.48
Al_2O_3	2.01	1.99	1.84	1.89
FeO	10.51	10.67	9.44	9.67
MnO	0.36	0.41	0.3	0.32
MgO	14.02	14.19	15.05	15.01
CaO	18.64	18.85	19.03	18.56
Na_2O	0.26	0.26	0.25	0.23
K_2O	n.d.	n.d.	n.d.	n.d.
TiO_2	0.62	0.61	0.35	0.31
Cr_2O_3	n.d.	0.02	0.14	0.15
Total	96.97	97.28	98.17	97.61
N. Ox.	6	6	6	6
Si	1.95	1.94	1.96	1.96
IVAl	0.05	0.07	0.04	0.04
VIAl	0.04	0.03	0.04	0.04
Fe(II)	0.34	0.34	0.3	0.31
Mn	0.01	0.01	0.01	0.01
Mg	0.81	0.81	0.85	0.85
Ca	0.77	0.78	0.77	0.76
Na	0.02	0.02	0.02	0.02
K	n.d.	n.d.	n.d.	n.d.
Ti	0.02	0.02	0.01	0.01
Cr	n.d.	n.d.	n.d.	0.01
∑ Cations	4	4	4	4
%Wo	39.97	39.9	40.00	39.29
%En	41.83	41.79	44.01	44.2
%Fs	18.2	18.31	15.99	16.51
%Fm	0.3	0.3	0.27	0.27

Total Fe reported as FeO. N. Ox. corresponds to the number of oxygen atoms per formula unit.

given in Table 3 and plotted in Fig. 4a and b in terms of interlayer cations IC (IC = Na + Ca + K) versus Si content and non-interlayer cations NIC (NIC = Si + Ti + Al_{total} + Fe + Mg + Mn) versus Al_{total} content, respectively. NIC values indicate that mafic phyllosilicates have compositions between chlorite and trioctahedral smectite. Corresponding to a mixed chlorite-smectite series, here named a Chl-Sm mixed-layer. The NIC displays a narrow range of values from 19.21 to 19.73 (Fig. 4b) whereas the sum of interlayered cations IC ranges between 0.034 and 0.311 (Fig. 4a) with a significant concentration in values below 0.15.

Calculation of the proportion of chlorite layers following the method of Wise (in Bettison and Schiffman, 1988) indicates that chlorite layer percentages range between 57 and 83%.

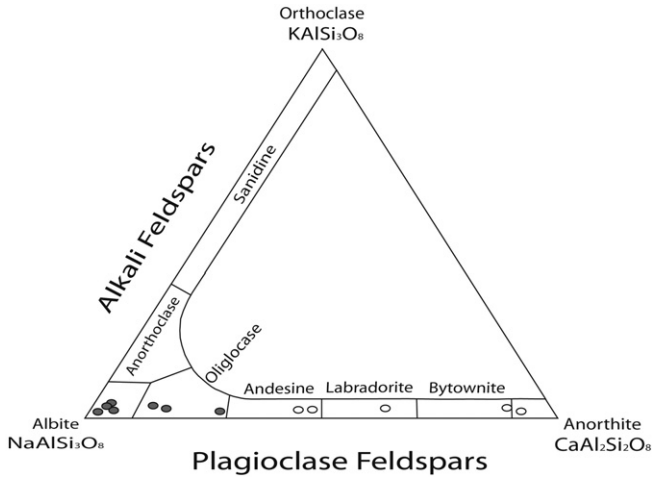

Fig. 3. Plagioclase compositions. White circles correspond to primary plagioclases, gray circles result from albitization.

4.2.3. Zeolites

Zeolites are found as partial or total replacement of primary plagioclase, or groundmass/matrix, and as vesicles, veins and veinlets infillings. Crystals show prismatic, radial and acicular habits corresponding to different types of zeolites. Representative zeolite compositions are given in Tables 4 and 5. The quality of the zeolite analyses can be estimated by means of a charge balance E% = ([100 * ((Al) − (Na + K) + 2 * (Mg + Ca + Sr + Ba)/(Na + K) + 2 * (Mg + Ca + Sr + Ba))]) which is 0 in a perfect analysis. The obtained E values are well above 0, probably because of the small grain size of the zeolite crystals.

Zeolite compositions obtained by EPMA were classified into two groups based on their difference of their silica content. Analyses with SiO_2 above 59% were grouped in a higher-silica content group (HSCG, Table 4), and those with SiO_2 below 55% in a lower-silica content group (LSCG, Table 5). HSCG microprobe analyses show geochemical affinities with stilbite, heulandite and clinoptilolite while those belonging to the LSCG closely match laumontite composition. Most of the analyses of the HSCG present a significant excess charge. Excess charge in heulandites has been recognized by many authors and is related to high Sr contents (e.g. Weisenberger and Selbekk, 2008). This characteristic is present in the samples from the HSCG and the LSCG and it is likely due to the not analyzed extra-framework elements such as Ba and Sr which are supposedly contained in all the zeolites from Hannah Point. Consequently, we validate the analyses of the HSCG and LSCG obtained in spite of the fact that most of them display E% values above 10% (see Tables 4 and 5).

The XRPD analyses indicate the presence of laumontite, stilbite, clinoptilolite, faujasite and phillipsite. These results partially agree with those found by EPMA, although it is likely that not all the analyses were performed on the same minerals given the considerable diversity of zeolites usually found in these rocks. The EPMA analyses show the chemical composition of the zeolites whereas XRD allows to determine a zeolite based on its characteristic crystallographic reflections. Three chemical classification diagrams based on pure end-member compositions of zeolites (Gottardi and Galli, 1985; Deer et al., 2004) were used to represent the EPMA data, and compare them with the XRD results.

The projection of the analyzed zeolites on the systems (0.5K)–(0.5Na)–(Ca) and (K)–(Na)–(Ca + Mg) in Fig. 5 displays similar trends for the LSCG and HSCG groups, with a high concentration of points close to the corners of Ca and Ca + Mg, indicating low K content and low to medium contents in Na. LSCG compositions exhibit a larger range of Na content than those of the HSCG. In both groups, LSCG and HSCG, projections fall into the compositional fields of laumontite, faujasite and stilbite (Fig. 5b, d). One sample from the LSCG in Fig. 5a and c plots in/adjacent to the clinoptilolite field.

The classification system 10(SiO_2/Al_2O_3)–(CaO + MgO)–(Na_2O + K_2O) in Fig. 6 shows a similar trend for the LSCG and HSCG analyses, displaying high concentrations in 10(SiO_2/Al_2O_3), low in (Na_2O + K_2O) and variable in (CaO + MgO). Most HSCG analyses plot in the heulandite field, although some of them present some minor affinities with stellerite, stilbite and epistilbite. One analysis from the HSCG with the lowest content in CaO + MgO of the group overlaps in three compositional spaces: clinoptilolite, mordenite and dachiardite. The LSCG analyses present good agreement with laumontite and weaker affinity with chabazite and wairakite.

In the light of the mayor affinities, the XRPD and EPMA analyses combined suggest that the HSCG has compositional affinities with heulandite, clinoptilolite, and stilbite, and the LSCG closely matches with laumontite compositions. Zeolites such as faujasite, mordenite, dachiardite or wairakite are not considered in the parageneses because of the absence of consistent data confirming their presence.

4.3. Very low-grade mineral paragenesis

The secondary minerals present correspond to: (a) albite ($Na_{0.98}Ca_{0.02}K_{0.00}$)$Al_{1.04}Si_{2.96}O_8$ close to the ideal end member

Table 2
Representative microprobe analyses of plagioclases from Late Cretaceous volcanic rocks at Hannah Point.

Sample	PEÑON	PEÑON	PEÑON	RBPB	RBPB	RBPB	RBPB	F12	ARC	ARC	ARC	ARC
SiO_2	57.56	58.22	67.66	44.25	45.79	59.52	67.36	67.41	56.48	67.13	60.04	61.82
Al_2O_3	26.51	26.21	20.34	35.1	32.86	22.96	20.13	20.26	27.23	20.37	20.3	19.4
FeO	0.33	0.34	0.08	0.5	1.03	1.74	0.02	0.04	0.39	0.01	4.45	4.12
MnO	n.d.	0.01	0	n.d.	0.02	0.02	0.01	n.d.	0.01	0.01	0.19	0.24
MgO	n.d.	0.01	0	0.14	0.48	0.48	0.01	0.01	0.02	n.d.	0.09	0.04
CaO	8.29	7.74	0.36	17.83	16.61	6.06	0.29	0.35	8.83	0.63	3.16	2.14
Na_2O	6.62	6.3	11.55	0.96	1.21	7.45	11.68	11.51	6.01	11.36	8.83	9.59
K_2O	0.33	1.2	0.02	0.01	0.03	0.42	0.03	0.04	0.24	0.03	0.51	0.42
TiO_2	0.01	0.02	0.02	0.01	0.02	0.07	0.01	0.01	0.02	n.d.	0.55	0.75
Cr_2O_3	n.d.	0.01	0.01	n.d.	0.01	n.d.	n.d.	0.01	0.01	n.d.	n.d.	n.d.
Total	99.65	100.05	100.03	98.8	98.06	98.73	99.54	99.64	99.25	99.54	98.13	98.5
N. Ox.	8	8	8	8	8	8	8	8	8	8	8	8
Si	2.59	2.61	2.96	2.07	2.16	2.72	2.96	2.96	2.55	2.95	2.79	2.86
Al	1.41	1.39	1.05	1.93	1.83	1.24	1.04	1.05	1.45	1.06	1.11	1.06
Fe	0.01	0.01	n.d.	0.02	0.04	0.07	n.d.	n.d.	0.01	n.d.	0.17	0.16
Ca	0.4	0.37	0.02	0.89	0.84	0.3	0.01	0.02	0.43	0.03	0.16	0.11
Na	0.58	0.55	0.98	0.09	0.11	0.66	1	0.98	0.53	0.97	0.8	0.86
K	0.02	0.07	n.d.	n.d.	n.d.	0.02	n.d.	n.d.	0.01	n.d.	0.03	0.02
∑ Cations	5.01	5	5.01	5.01	4.98	5	5.02	5.01	4.99	5.01	5.06	5.06
%An	40.12	37.61	1.71	91.04	88.16	30.25	1.36	1.67	44.16	2.99	15.99	10.69
%Ab	57.99	55.44	98.2	8.9	11.67	67.26	98.48	98.12	54.38	96.84	80.94	86.83
%Or	1.89	6.95	0.08	0.06	0.18	2.5	0.16	0.21	1.45	0.17	3.06	2.48

Total Fe reported as FeO. N. Ox. corresponds to the number of oxygen atoms per formula unit.

composition, (b) mafic phyllosilicates consisting of Chl-Sm mixed-layer with compositions ranging between 57–83% chlorite layers expressed as clinochlore: $(Mg, Fe^{2+})_5Al(Si_3Al)O_{10}(OH)_8$ mixed with 43–17% layers of trioctahedral smectite (saponite: $(Ca_{0.2}Na_{0.1})(Mg, Fe^{2+})_3(Si, Al)_4O_{10}(OH)_2\cdot 4(H_2O)$), (c) celadonite (ideal composition $K_2(Mg,Fe^{2+})_2(Al, Fe^{3+})_2Si_8O_{20}(OH)_4$ as defined by Buckley et al. (1978)), and (d) high silica and low silica content zeolites and calcite ($CaCO_3$).

Using the ideal compositions given by Coombs et al. (1997), the zeolites identified in this study would correspond to heulandite-Ca ($(Ca_{3.57}Sr_{0.05}Ba_{0.06}Mg_{0.01}Na_{1.26}K_{0.43})[Al_{9.37}Si_{26.70}O_{72}]\cdot 26.02H_2O$), stilbite ($(Ca_{0.5},Na,K)_9[Al_9Si_{27}O_{72}]\cdot 28H_2O$), clinoptilolite-Ca ($(Na_{1.76}K_{1.05}Ca_{1.90}Mg_{0.17})[Al_{6.72}Si_{29.20}O_{72}]\cdot 23.7H_2O$), all from the HSCG and laumontite ($Ca_4[Al_8Si_{16}O_{48}]\cdot 18H_2O$) the only zeolite from the LSCG.

5. Chlorite geothermometry

In general terms, chlorite is a phyllosilicate showing a wide range of composition and it can be represented by the generic formula:

$$\left(R_u^{2+} + R_y^{3+} + X_z\right)^{VIII}\left(Si_{4+x}Al_x\right)^{IV} O_{10+w}\,(OH)_{8-w},$$

where $u + y + z = 6$, and $z = \dfrac{y-w-x}{2}$.

R^{2+} represents divalent ions (Mg^{2+} or Fe^{2+}); R^{3+} stands for trivalent ions (Al^{3+} or Fe^{3+}); y and x denote the degree of substitution of

Table 3
Representative microprobe analyses of mafic phyllosilicates from Late Cretaceous volcanic rocks at Hannah Point.

Sample	SN	SN	SN	SN	SN	SN	09.06.2006	09.06.2006	09.06.2006	09.06.2006	09.06.2006
SiO_2	32.08	33.27	31.73	34.08	31.91	33.48	30.85	32.29	31.12	31.12	31.85
Al_2O_3	14,.4	15.07	14.58	13.93	13.87	14.72	13.76	14.46	14.85	14.34	15.40
FeO	19.58	18.67	19.81	19.02	19.85	19.17	22.37	22.42	23.62	23.74	22.98
MnO	0.45	0.38	0.39	0.36	0.41	0.40	0.40	0.40	0.37	0.42	0.36
MgO	20.95	19.09	20.25	18.91	20.12	20.21	16.91	17.42	17.52	17.52	16.32
CaO	0.14	0.77	0.20	0.66	0.43	0.79	0.36	0.34	0.28	0.34	0.39
Na_2O	0.01	0.06	0.01	0.01	0.02	0.01	n.d.	0.01	0.02	0.01	0.02
K_2O	n.d.	0.02	n.d.	0.64	0.01	0.03	0.03	0.03	0.01	0.02	0.01
TiO_2	0.02	n.d.	0.01	0.01	0.01	n.d.	0.01	0.02	0.02	0.01	0.01
Cr_2O_3	n.d.	n.d.	n.d.	n.d.	n.d.	n.d.	0.02	n.d.	0.02	0.01	n.d.
Total	87.27	87.33	86.98	87.62	86.63	88.81	84.71	87.39	87.83	87.53	87.34
N. Ox.	28	28	28	28	28	28	28	28	28	28	28
Si	6.55	6.73	6.51	6.90	6.58	6.68	6.61	6.67	6.45	6.49	6.59
Ti	n.d.	n.d.	n.d.	n.d.	n.d.	n.d.	n.d.	n.d.	n.d.	n.d.	n.d.
IVAl	1.45	1.27	1.49	1.10	1.42	1.32	1.39	1.33	1.55	1.51	1.41
VIAl	1.93	2.32	2.03	2.22	1.95	2.14	2.08	2.19	2.08	2.01	2.35
Cr(III)	n.d.	n.d.	n.d.	n.d.	n.d.	n.d.	n.d.	n.d.	n.d.	n.d.	n.d.
Fe(II)	3.34	3.16	3.40	3.22	3.42	3.20	4.01	3.87	4.10	4.14	3.98
Mn(II)	0.08	0.06	0.07	0.06	0.07	0.07	0.07	0.07	0.07	0.07	0.06
Mg	6.38	5.76	6.19	5.71	6.18	6.01	5.40	5.36	5.42	5.44	5.04
Ca	0.03	0.17	0.04	0.14	0.10	0.17	0.08	0.07	0.06	0.08	0.09
Na	n.d.	0.02	n.d.	n.d.	0.01	0.01	n.d.	n.d.	0.01	n.d.	0.01
K	n.d.	n.d.	n.d.	0.16	n.d.	0.01	0.01	0.01	n.d.	n.d.	n.d.
NIC	19.73	19.30	19.68	19.21	19.63	19.42	19.57	19.49	19.66	19.67	19.43
IC	0.03	0.20	0.05	0.31	0.11	0.18	0.09	0.09	0.07	0.09	0.10
Xc	0.83		0.81		0.79		0.75	0.71	0.80	0.80	0.68
T [°C] Cathelineau (1988)	172		178		167		162	152	188	181	165

Total Fe reported as FeO. N. Ox. corresponds to the number of oxygen atoms per formula unit.
Xc corresponds to the percentage of chlorite

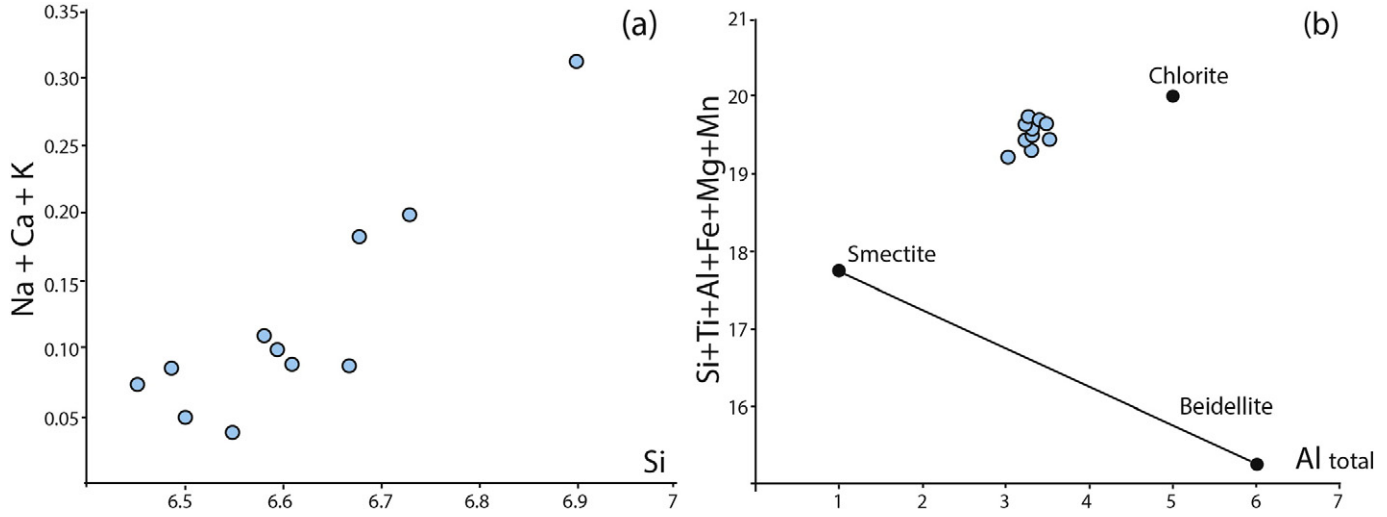

Fig. 4. Composition of mafic phyllosilicates from Hanna Point calculated at 28 oxygens. (a) IC (interlayer cations: Na + Ca + K) vs Si/28 oxygens. (b) NIC (non-interlayer cations: Si + Ti + Al_{total} + Fe + Mg + Mn) vs Al_{total}.

trivalent cations in the octahedral (VI) and tetrahedral (IV) sheets respectively, *z* accounts for structural vacancies (X); and *w* is generally 0 or a small number (e.g. de Caritat et al., 1993).

Several geothermometers for chlorite have been proposed based on the octahedral vacancies, tetrahedral aluminum (Al^{IV}) amount and X_{Fe} content, among others factors (see review of de Caritat et al., 1993). We have applied Cathelineau's chlorite geothermometer (1988), the most widely used, to the samples from Hannah Point. This author proposed an empirical relationship between the amount of tetrahedral aluminum (Al^{IV}) in chlorites and their temperature of formation given by the following expression:

$$T[^{\circ}C] = -61.392 + 321.98 * Al^{IV}.$$

In the application of this method we have considered only those mafic phyllosilicates with a chlorite layer percentage above 75% in order to have trustful temperatures, which yielded temperatures values between 162 and 192 °C.

6. Discussion

6.1. Secondary mineral association

The XRPD and EPMA data compared with known mineral compositions point to the presence of laumontite, stilbite, heulandite and clinoptilolite. The possible occurrence of phillipsite and faujasite indicated by XRPD, although not supported by the EPMA results, has not been considered in this discussion.

Mafic phyllosilicates have compositions between chlorite and trioctahedral smectite, with diabantite affinity i.e. they correspond to Chl-Sm mixed-layer. Celadonite is recognized in a few samples without a clear pattern of occurrence. Although analyses of mafic phyllosilicates are scarce, the uniform composition displayed by them in the transition from trioctahedral smectite to chlorite (Fig. 4b) probably indicates at least local equilibrium.

Notably absent in the Hannah Point volcanic rocks are the common very-low grade metamorphic minerals epidote, pumpellyite and prehnite. This would indicate temperatures and pressures falling below the stability fields of these calc-silicate phases although a control from rock chemical composition and the nature of the hydrothermal fluids is also possible (e.g. Miron et al., 2012).

6.2. Thermobarometric conditions

Two evidences suggest that the very low-grade alteration observed at Hannah Point occurred at low pressures. First, the 500 m minimum thickness of the volcanic succession corresponds to a minimum lithostatic pressure of ca. 0.1 kbar for typical andesitic to basaltic lava densities. Second, prehnite-pumpellyite facies assemblages are absent in these rocks, suggesting a maximum lithostatic pressure of ca. 2 kbar equivalent to ca. 8 km (e.g. Frey et al., 1991). Considering the absence of a higher pressure paragenesis it is geologically difficult to conceive an amount of erosion of the sequence of about 7 km. Therefore we conclude that the alteration at Hannah Point occurred at pressures much lower than 2 kbar and greater than 0.1 kbar.

Experimental work by Liou et al. (1991) and field observations in Iceland by Kristmannsdóttir (1979) show that laumontite formed at temperatures above ca. 150 °C and according to Fridriksson et al. (2001), laumontite plus quartz is stable above ca. 125 °C. The petrogenetic grid of Frey et al. (1991) indicates that laumontite is stable in the range of approximately 180–260 °C and Liou et al. (1991) determined the upper temperature limit of laumontite to be about 260 °C below 1000 bars. According to Frey et al. (1991) heulandite is restricted to low pressures (<1800 bars) and temperatures below about 230 °C. Liou et al. (1991) indicate that formation of heulandites would require a minimum pressure of 600 bars, which might be a lower pressure limit. Stilbite, according to Liou et al. (1991), is stable below 150 °C, whereas Frey et al. (1991) indicate an upper temperature limit of about 180 °C. According to Liou et al. (1991) the assemblages albite + laumontite and heulandite + clinoptilolite are stable at temperatures below 200 °C, which can be considered here as an upper temperature limit assemblage. This information allows to estimate of the formation temperature of the mineral association laumontite + heulandite + stilbite + clinoptilolite + albite as comprised in the interval 150 and 200 °C. Also, the formation pressures of the same mineral association would fall in the range 600–1800 bars. Interestingly, the minimum formation pressure of 600 bars and the present 500 m thickness reported for the volcanic pile (exercising 0.1 bar pressure) suggest that the Late Cretaceous succession at Hannah Point has been eroded at least 1 km in thickness.

6.3. Fluids and the alteration model

The chemical characteristics of the secondary minerals in rocks of Hannah Point indicate that the alteration processes required a

Table 4
Representative microprobe analyses of HSCG zeolites from Late Cretaceous volcanic rocks at Hannah Point.

	Clinoptilolite	Stilbite	Stilbite	Heulandite	Heulandite	Heulandite	Heulandite	Heulandite	Heulandite	Heulandite	Heulandite	Heulandite	Heulandite	Heulandite
SiO_2	65.91	59.67	59.32	66.37	65.99	65.49	64.6	64.19	63.63	63.52	63.28	63.2	61.13	60.81
TiO_2	0.01	n.d.	n.d.	0.02	n.d.	n.d.	n.d.	0.01	0.02	0.01	n.d.	n.d.	0.01	n.d.
Al_2O_3	13.69	16.7	16.61	14.04	14.67	13.34	13.02	13.91	14.94	14.73	15.45	13.53	16.05	16.32
Cr_2O_3	n.d.	0.01	n.d.	n.d.	0.01	0.02	n.d.	n.d.	n.d.	n.d.	n.d.	n.d.	0.02	0.01
FeO	0.04	0.09	0.04	0.05	0.06	0.03	0.02	0.24	0.08	0.21	0.16	0.03	0.03	0.03
MnO	n.d.	n.d.	0.01	n.d.	n.d.	0.01	n.d.	0.01	n.d.	n.d.	n.d.	n.d.	n.d.	n.d.
MgO	n.d.	0.01	n.d.	0.08	0.01	n.d.	n.d.	n.d.	0.04	0.02	0.66	0.01	n.d.	0.03
CaO	3.51	6.59	6.32	5.29	5.63	4.8	5.36	5.76	5.58	6.04	5.7	4.75	6.14	6.47
Na_2O	2.64	0.28	0.79	1.14	0.96	1.66	0.82	0.34	1.2	0.15	0.5	2.61	0.71	1.02
K_2O	0.19	0.52	0.5	0.33	0.38	0.54	0.35	0.42	0.28	0.39	0.3	0.43	0.52	0.44
Total	86	83.89	83.6	87.32	87.73	85.88	84.18	84.88	85.78	85.07	86.06	84.57	84.6	85.13
Si	29.2	27.42	27.39	29.01	28.76	29.16	29.25	28.87	28.42	28.54	28.15	28.75	27.8	27.58
Ti	n.d.	n.d.	n.d.	0.01	n.d.	n.d.	n.d.	n.d.	0.01	n.d.	n.d.	n.d.	n.d.	n.d.
Al	7.15	9.05	9.04	7.23	7.53	7	6.95	7.37	7.86	7.8	8.1	7.25	8.61	8.72
Fe(III)	0.01	0.04	0.02	0.02	0.02	0.01	0.01	0.09	0.03	0.08	0.06	0.01	0.01	0.01
Cr(III)	n.d.	n.d.	n.d.	n.d.	n.d.	0.01	n.d.	n.d.	n.d.	n.d.	n.d.	n.d.	0.01	n.d.
Mn(II)	n.d.	n.d.	n.d.	n.d.	n.d.	n.d.	n.d.	n.d.	n.d.	n.d.	n.d.	n.d.	n.d.	n.d.
Mg	n.d.	0.01	n.d.	0.05	0.01	n.d.	n.d.	n.d.	0.03	0.01	0.44	0.01	n.d.	0.02
Ca	1.67	3.25	3.13	2.48	2.63	2.29	2.6	2.78	2.67	2.91	2.72	2.32	2.99	3.14
Na	2.27	0.25	0.71	0.97	0.81	1.43	0.72	0.3	1.04	0.13	0.43	2.3	0.62	0.89
K	0.11	0.31	0.3	0.18	0.21	0.3	0.2	0.24	0.16	0.22	0.17	0.25	0.3	0.25
N. Ox.	72	72	72	72	72	72	72	72	72	72	72	72	72	72
$\sum$ Cations	40.41	40.33	40.59	39.95	39.97	40.2	39.73	39.65	40.22	39.69	40.07	40.89	40.34	40.61
E%	25.55	28.44	24.68	16.74	20.04	11.04	13.46	22.4	19.7	27.27	18.01	0.93	24.7	16.86
Si/(Si + Al)	0.8	0.75	0.75	0.8	0.79	0.81	0.81	0.8	0.78	0.79	0.78	0.8	0.76	0.76
Ca/(Ca + Na + K)	0.41	0.85	0.76	0.68	0.72	0.57	0.74	0.84	0.69	0.89	0.82	0.48	0.76	0.73

Total Fe reported as Fe_2O_3. N. Ox. corresponds to the number of oxygen atoms per formula unit. $\sum$ Cations correspond to the total sum of the cations.

Table 5
Representative microprobe analyses of LSCG zeolites from Late Cretaceous volcanic succession at Hannah Point.

	Laumontite	Laumontite	Laumontite	Laumontite	Laumontite
SiO_2	50.65	54.52	54.46	53.91	53.59
TiO_2	n.d.	n.d.	n.d.	0.03	n.d.
Al_2O_3	21.09	21.11	21.43	22.03	21.06
Cr_2O_3	0.01	n.d.	0.01	n.d.	n.d.
FeO	2.91	0.09	0.03	0.04	0.13
MnO	0.06	n.d.	n.d.	n.d.	n.d.
MgO	0.72	n.d.	n.d.	n.d.	n.d.
CaO	8.72	10.19	9.81	10.14	10.23
Na_2O	0.89	0.49	1.08	0.19	0.42
K_2O	0.29	0.33	0.36	0.36	0.38
Total	85.35	86.73	87.18	86.7	85.82
Si	15.81	16.55	16.48	16.36	16.47
Ti	n.d.	n.d.	n.d.	0.01	n.d.
Al	7.76	7.55	7.64	7.88	7.63
Fe(III)	0.76	0.02	0.01	0.01	0.03
Cr(III)	n.d.	n.d.	n.d.	n.d.	n.d.
Mn(II)	0.02	n.d.	n.d.	n.d.	n.d.
Mg	0.33	n.d.	n.d.	n.d.	n.d.
Ca	2.92	3.32	3.18	3.3	3.37
Na	0.54	0.29	0.63	0.11	0.25
K	0.12	0.13	0.14	0.14	0.15
N. Ox.	48	48	48	48	48
$\sum$ Cations	28.26	27.86	28.08	27.81	27.9
E%	19	7.51	7.21	15.27	7.4
Si/(Si + Al)	0.67	0.69	0.68	0.67	0.68
Ca/(Ca + Na + K)	0.82	0.89	0.81	0.93	0.89

Total Fe reported as Fe_2O_3. N. Ox. corresponds to the number of oxygen atoms per formula unit. $\sum$ Cations correspond to the total sum of the cations.

significant amount of H_2O. The anhydrous primary mineralogy of the volcanic rocks was partially to totally replaced by a hydrous secondary mineralogy. The occurrence of alteration minerals in amygdules, veins and veinlets indicates that hot water circulated through open spaces interacting with the rock. Aqueous fluids derived from this interaction would have produced the Ca-Al silicates, mainly zeolites, in the volcanic succession. Fluid-driven chemical reactions progressed from the open spaces inward of the rocks through the porosity resulting from the process. Aqueous fluids invaded the groundmass contributing to the formation of patches of secondary minerals.

The rounded shape of the amygdules shows that no ductile deformation took place before and/or during the alteration process. Veins and veinlets, at different scales, filled by secondary minerals are evidence of brittle deformation during the development or cooling of the alteration event. The involvement of aqueous fluids and fracturing by brittle deformation are characteristic features of hydrothermal alteration. Consequently, hydrothermal processes are thought as the main factor responsible for the occurrence of the alteration minerals. Textural and mineralogical features observed in amygdules, veins and veinlets suggest at least three successive paragenetic stages: (1) celadonite/mafic phyllosilicates, (2) zeolites and (3) calcite. These three stages may depict the spatial and temporal development of secondary mineral assemblages in the volcanic succession at Hannah Point.

Stage 1 represents the earliest alteration and is characterized by rims of mafic phyllosilicates (Chl-Sm mixed-layer, see Fig. 2b, c) and minor celadonite in the amygdule. The chemical components necessary for the precipitation of Chl-Sm mixed-layer are, in this case, mainly derived from hydrolysis of pyroxene, olivine and basaltic/andesitic glass. Mg, Fe, Si, Al and minor Ca and Na would have been remobilized by the dissolution of chemical components by the aqueous fluids and then precipitated in open spaces and/or original minerals. K, very scarce in the original lavas, would have been added to the primary chemical system by the external aqueous fluids. This mafic phyllosilicate formation mechanism has been related to burial processes as the main responsible for reaching the paragenetic conditions (e.g. Levi et al., 1989; Aguirre et al., 1989; Alt, 1999; Robinson and Bevins, 1999).

Stage 2 is characterized by the presence of zeolites with typical euhedral habit located at the center of the amygdules or in veins and veinlets. The albitization of the primary plagioclase at Hannah Point occurred with minimal disruption of primary textures, Ca and Na were remobilized by this process resulting in Ca-enrichment of the fluids circulating in the rock-system. The increase of the Ca chemical potential would result in stabilizing mineral assemblages containing Ca-rich zeolites such as laumontite, stilbite and heulandite. This mechanism of zeolite formation is considered a fundamental feature in this type of alteration processe in very low-grade metabasites (e.g. Liou et al., 1991).

Stage 3 is characterized by the presence of large anhedral crystals of calcite which suggests that the CO_2 concentrations in the late fluids were moderate to high. The absence of zeolites at this stage can be explained by the fact that zeolites are stable in water with a low CO_2 concentration. The increasing of the chemical potential of CO_2 relative to that of H_2O results in the stability of the assemblages containing calcite, quartz and clay minerals. This suggests that the chemical evolution of the fluids during the formation of the secondary mineral assemblages might be characterized by a transition from early aqueous fluids to late CO_2-rich fluids.

6.4. Paragenetic model and its possible correlation with the Icelandic model and others extensional settings

Located on the mid-Atlantic Ridge, Iceland is part of the mid-ocean ridge system, consisting of flood basalts volcanoes ranging in age from 16 Ma to the present (Palmason et al., 1979). The occurrence of very low-grade assemblages in the Icelandic rocks is a widespread phenomenon. The modern origin of the very-low grade metamorphism of the Icelandic rocks has permitted researchers to observe features which might not be possible to find in other extensional basins (e.g. Andean Basins).

The most accepted alteration model for the Icelandic volcanics involves regional burial metamorphism superimposed by a later hydrothermal activity associated with the magmatism of the active rift zone (Palmason et al., 1979). Based on homogenization temperatures on fluid inclusions in calcite, chlorite geothermometry and the mineralogical-textural associations, the very low-grade mineral assemblages have been correlated with different metamorphic events (e.g. Neuhoff et al., 1999; Weisenberger and Selbekk, 2008). In general the first stage is related to the burial of the volcanic pile and is characterized by rims of chlorite/smectite filling porosities. A second stage follows after the burial stage and is related to a widespread occurrence of zeolites filling open spaces and also replacing phenocrysts. This stage corresponds to hydrothermal alteration associated with the intrusion of basaltic dikes. Most of these features are also been documented in other extensional settings such as the Andean Basins (e.g. Aguirre, 1993) or the North Shore Volcanic Group at Minnesota (e.g. Schmidt, 1993)

A possible correlation in terms of genetic processes between the very low-grade mineral assemblages at Hannah Point and those present in the Icelandic rocks (e.g. Neuhoff et al., 1999) is given by the identification of these three stages: (1) celadonite/mafic phyllosilicates, (2) zeolites and (3) calcite.

Although the very low-grade mineral assemblages were produced in rocks of different geochemical affinities in Iceland and the South Shetlands Islands, tholeitic and calc-alkaline respectively, the similarities in terms of mineralogy and textural occurrence are worth mentioning. Nevertheless, there are still important factors to clarify in this correlation such as the identification of the hydrothermal event(s) responsible for the mineral phases of the second and third stage present in the rocks of Hanna Point considering that the volcanic activity recorded in Livingston Island has been continuous for at least 60 Ma, from the Late Cretaceous to the Tertiary (Haase et al., 2012).

7. Conclusions

The Late Cretaceous volcanic succession at Hannah Point presents secondary mineral associations characteristic of very low-grade

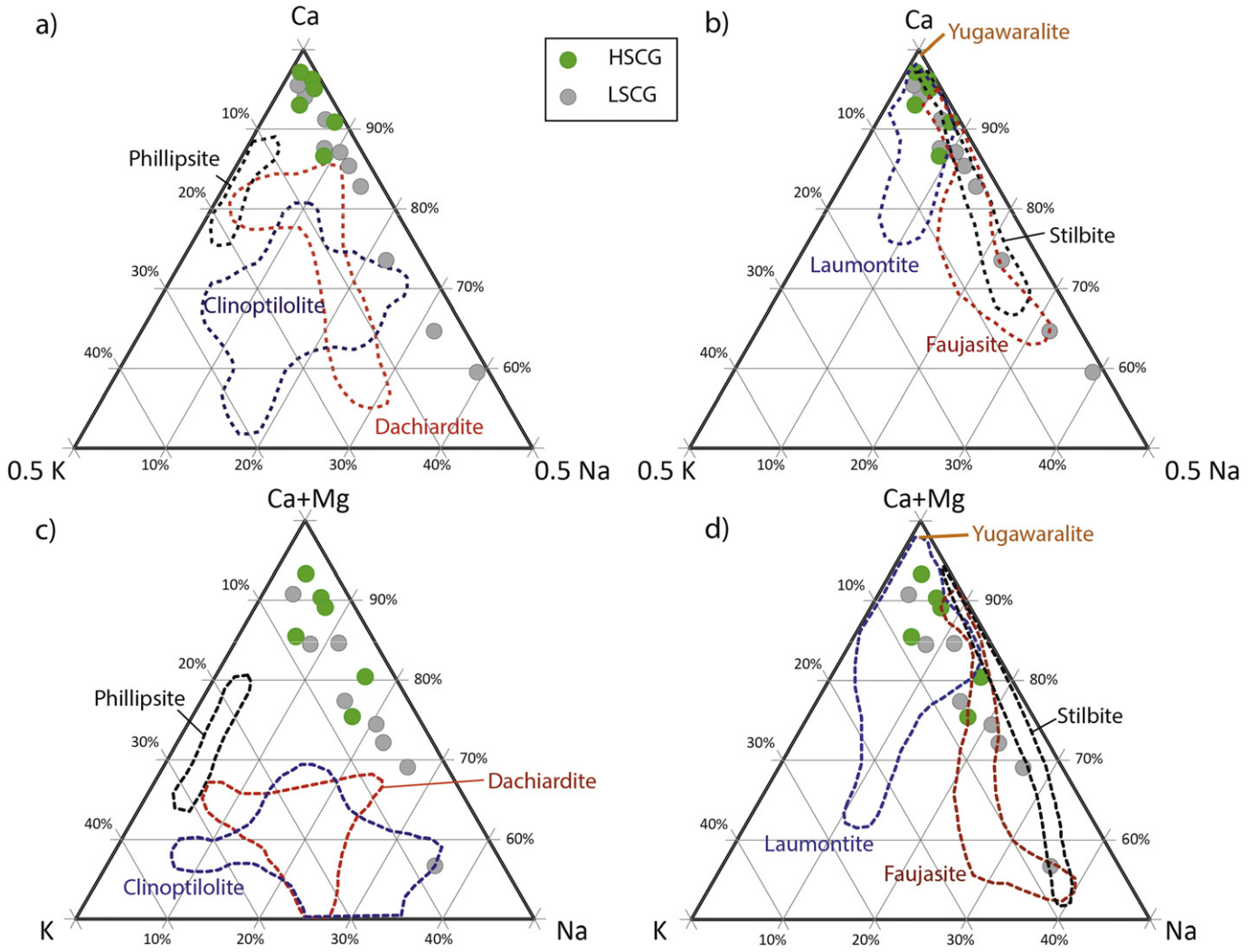

Fig. 5. Projection of the analyzed zeolites on the chemical systems: (0.5K)–(0.5Na)–(Ca), (a) and (b), and (K)–(Na)–(Ca + Mg), (c) and (d). HSCG: higher-silica content group. LSCG: lower-silica content group. Dotted fields correspond to the compositions of zeolites collected by the authors from various works published in international journals (e.g. Gottardi and Galli, 1985, Deer et al., 2004, Fuentes et al., 2004) and identified by XRD and EPMA analyses.

metamorphism. The minerals occur in fractures (veins and veinlets), amygdules, groundmass/matrix and phenocrysts. The paragenesis corresponds to albite, mafic phyllosilicates, zeolites, celadonite and calcite. The primary magmatic plagioclase has a compositional range between $An_{91}Ab_{09}$ and $An_{55}Ab_{45}$ whereas secondary albite ranges between $An_{02}Ab_{98}$ and $An_{28}Ab_{72}$. The mafic phyllosilicates consist from an interlayering between chlorite and trioctahedral smectite, the chlorite layer percentages ranging between 57% and 84%, and displaying diabantitic compositions. Among the zeolites, high silica content (heulandite, clinoptilolite and stilbite) and low silica content (laumontite) groups have been identified.

According to chlorite geothermometers and the known stability temperatures of the paragenetic mineral assemblages, we estimate that the temperature of the alteration event ranged between 150 and ~200 °C whereas pressure was in the range 600–1800 bars. This suggest that the Upper Cretaceous volcanic succession at Hannah Point has been eroded at least 1 km to the present day thickness.

The albitization of the primary Ca-rich plagioclases contributed to the formation of Ca-rich fluids, which pervaded the rock-system resulting in the generation of Ca-rich zeolites, and calcite. Mafic phyllosilicates and celadonite occur usually as a rim at the wall of the amygdules, probably due to the hydrolysis of olivine, pyroxene and basaltic glass. Aqueous fluids from which zeolites precipitated had compositions mainly characterized by the dissolved chemical elements Ca, Na, Mg, Fe, Al and Si. The alteration process required a significant amount of H_2O and K, which could have been provided by external aqueous fluids.

Three distinct paragenetic stages were identified: (1) celadonite/mafic phyllosilicates, (2) zeolites and (3) calcite. Stage 1 was formed during burial metamorphism, followed by stages 2 and 3 generated during hydrothermal alteration related to magmatic events. A chemical evolution of the fluids from early aqueous fluids towards late CO_2-rich fluids is apparent.

The mineral occurrence and textural relations of the different stages are similar to those described in Iceland, where the chlorite/smectite rim assemblages of the amygdules point to burial metamorphism, while those present in the core of the amygdules and filling veins and veinlets point to hydrothermal alteration. All these characteristics make it reasonable to sustain a regional burial metamorphism superimposed by hydrothermal alteration as the origin of the very low-grade mineral associations present in the rocks of Hannah Point.

The mineral evolution in the very-low grade metamorphism that we propose here can be used in the prospection of geothermal renewable energy. Differences established with very low-grade mineral associations provide useful mineral indicators particularly in the case of geothermal exploration.

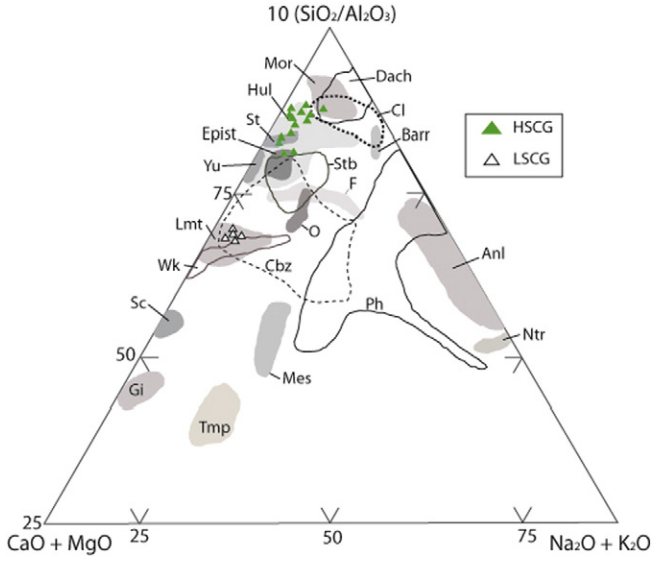

Fig. 6. Projection of the analyzed zeolites on the chemical system $10(SiO_2/Al_2O_3)$–$(CaO + MgO)$–$(Na_2O + K_2O)$ used for the classification of zeolites. Fields of zeolite compositions were outlined using the data base from various authors published in international journals (e.g. Gottardi and Galli, 1985, Deer et al., 2004, Fuentes et al., 2004). Abbreviations of minerals after Kretz (1983): Hul = heulandite, Lmt = laumontite, Stb = stilbite, Cbz = chabazite, Anl = analcime, Ntr = natrolite, Tmp = thomsonite, Dach = dachiardite, Mor = mordenite, Cl = clinoptilolite, Barr = barrerite, St = stellerite, Yu = yugawaralite, Epist = epistilbite, F = faujasite, O = offretite, Wk = wairakite, Lev = levyne, Ph = phillipsite, Go = gobbinsite, Ga = garronite, Sc = scolecite, Gi = gismondine, Mes = mesolite, Am = amicite.

Acknowledgments

The authors would like to thank the three anonymous reviewers for their helpful comments and valuable suggestions. The samples were collected by Walter Michea & Marcelo Leppe. This research was supported by the projects G1409, ACT-105, and RT0614 funded by the Chilean Antarctic Institute (INACH) and Comisión Nacional de Investigación Científica y Tecnológica (CONICYT). The authors would like to thank Dra. Eugenia Fonseca for the XRD analyses performed at the Servicio Nacional de Geología y Minería (SERNAGEOMIN), Chile.

References

Aguirre, L., 1993. Compositional variations of Cretaceous pumpellyites along the western margin of South America and their relation to an extensional geodynamic setting. J. Metamorph. Petrol. 11, 437–448.

Aguirre, L., Levi, B., Nystrom, J.O., 1989. The link between metamorphism, volcanism and geotectonic setting during the evolution of the Andes. Geol. Soc. Lond. Spec. Publ. 43 (1), 223–232.

Alt, J.C., 1999. Very low-grade hydrothermal metamorphism of basic igneous rocks. In: Frey, M., Robinson, D. (Eds.), Low-grade Metamorphism. Wiley-Blackwell, Ltd., London, pp. 170–201 (Chapter Chapter 6).

Araya, R., Hervé, F., 1965. Estudio geomorfológico y geológico en las Islas Shetands del Sur, Antártica. Publicaciones Instituto Antártico Chileno 8 pp. 1–17.

Bastias, J., Fuentes, F., Aguirre, L., Hervé, F., Fernandoy, F., Demant, A., 2013. Zeolites and mafic phyllosilicates in Livingston Island, Antarctica. Goldschmidt 2013 Conference Abstracts, p. 666.

Bastias, J., Hervé, F., 2013. The Cape Wallace Beds: a Permian: detritus turbidite unit at Low Island, South Shetland Islands. Boll. Geofis. Teor. Appl. 54 (Suppl. 2), 312–314.

Bastias, J., 2014. Mineralogía y geocronología U-Pb en las Islas Shetland del Sur, Antártica, un multienfoque para Punta Hannah, Isla Livingston y Cabo Wallace, Isla Low (Ms Thesis) Geology Department, Universidad de Chile, Santiago (http://www.repositorio.uchile.cl/handle/2250/115611).

Barker, P.F., 1982. The Cenozoic subduction history of the Pacific margin of the Antarctic Peninsula: ridge crest-trench interactions. J. Geol. Soc. 139, 787–801.

Bettison, L.A., Schiffman, P., 1988. Compositional and structural variation of the phyllosilicates from the Point Sal Ophiolite, California. Am. Mineral. 73, 62–76.

Buckley, H.A., Bevan, J.C., Brown, K.M., Johnson, L.R., Farmer, V.C., 1978. Glauconite and celadonite: two separate mineral species. Mineral. Mag. 42, 373–382.

Castillo, P., Fanning, M., Hervé, F., Lacassie, J.P., 2015. Characterisation and tracing of Permian magmatism in the south-western segment of the Gondwanan margin; U–Pb age, Lu–Hf and O isotopic compositions of detrital zircons from metasedimentary complexes of northern Antarctic Peninsula and western Patagonia. Gondwana Res. http://dx.doi.org/10.1016/j.gr.2015.07.014.

Cathelineau, M., 1988. Cation site occupancy in chlorites and illites as a function of temperature. Clay Miner. 23, 471–485.

Coombs, D.S., Alberti, A., Armbruster, T., Artioli, G., Colella, C., Galli, E., Grice, J.D., Liebau, F., Mandarino, J.A., Minato, H., Nickel, E.H., Passaglia, E., Peacor, D.R., Quartieri, S., Rinaldi, R., Ross, M., Sheppard, R.A., Tillmanns, E., Vezzalini, G., 1997. Recommended nomenclature for zeolite minerals: report of the subcommittee on zeolites of the International Mineralogical Association, Commission on New Minerals and Mineral Names. Can. Mineral. 35, 1571–1606.

De Caritat, P., Hutcheon, I., Walshe, J.L., 1993. Chlorite geothermometry: a review. Clay Clay Miner. 41, 219–239.

Deer, W.A., Howie, R.A., Wise, W.S., Zussman, J., 2004. Volume 4B. Framework Silicates: Silica Minerals, Feldespathoids, and the Zeolites. The Geological Society, Rock-Forming Minerals, Volume 48, London.

Frey, M., De Captani, D., Liou, J.G., 1991. A new petrogenetic grid for low-grade alteration metabasites. J. Metamorph. Geol. 9, 497–509.

Fridriksson, T., Neuhoff, P., Arnorsson, S., Bird, D., 2001. Geological constraints on the thermodynamic properties of the stilbite-stellerite solid solution in low-grade metabasalts. Geochim. Cosmochim. Acta 65, 3993–4008.

Fuentes, F., Aguirre, L., Vergara, M., Valdebenito, L., Fonseca, E., 2004. Miocene fossil hydrothermal system associated with a volcanic complex in the Andes of central Chile. J. Volcanol. Geotherm. Res. 138, 139–161.

Fuentes, F., Chavez, G., Bastias, J., Aguirre, L., Aguirre, L., 2015. Very low-grade hydrothermal metamorphism of Cenozoic volcanics in Fildes Peninsula, King George Island, Antarctica. Goldschmidt 2015 Abstracts, p. 963.

Gracanin, T.M., 1983. Geochemistry and Geochronology of Some Mesozoic Igneous Rocks From the Northern Antarctic Peninsula Region M. Sc. Thesis Ohio State University.

Grunow, A., Dalziel, I., Harrison, T.M., Heizler, M., 1992. Structural geology and geochronology of subduction complexes along the margin of Gondwanaland: new data from the Antarctic Peninsula and southernmost Andes. Geol. Soc. Am. Bull. 104, 1497–1514.

Gottardi, G., Galli, E., 1985. Natural Zeolites. Springer, Minerals and Rocks, New York-Tokyo.

Haase, K.M., Beier, C., Fretzdorff, S., Smellie, J.L., Garbe-Schönberg, 2012. Magmatic evolution of the South Shetland Islands, Antarctica, and implications for continental crust formation. Contrib. Mineral. Petrol. 163 (6), 1103–1119.

Hervé, F., Miller, H., Pimpirev, C., 2005. Patagonia–Antarctica connections before Gondwana break-up. In: Fütterer, D., Damaske, D., Kleinschmidt, G., Miller, H., Tessensohn, F. (Eds.), Antarctica: Contribution to Global Earth Sciences. Springer Verlag, pp. 217–228 (Chapter 5.1).

Hervé, F., Faundez, V., Brix, M., Fanning, C.M., 2006. Jurassic sedimentation of the Miers Bluff Formation, Livingston Island, Antarctica: evidence from SHRIMP U–Pb ages of detrital and plutonic zircons. Antarct. Sci. 18 (2), 229–238.

Kretz, R., 1983. Symbols of rock-forming minerals. Am. Mineral. 68, 309–343.

Kristmannsdóttir, H., 1979. Alteration of basaltic rocks by hydrothermal activity at 1008–300 8C. In: Mortland, M., Farmer, V. (Eds.), Developments in Sedimentology. Elsevier, Amsterdam, pp. 359–367 (Volume 27).

Leat, P., Scarrow, J., Millar, I., 1995. On the Antarctic Peninsula batholith. Geol. Mag. 132 (4), 399–412.

Leppe, M., Michea, W., Muñoz, C., Palma-Heldt, S., Fernandoy, F., 2007. Paleobotany of Livingston Island: the first report of a Cretaceous fossil flora from Hannah Point. In: Cooper, A.K., Raymond, C.R. (Eds.), Antarctica: A Keystone in a Changing World. U.S. Geological Survey and the National Academies, USGS OF-2007-1407, Short Research Paper 081. http://dx.doi.org/10.3133/of2007-1047.srp081.

Levi, B., Aguirre, L., Nystrom, J.O., Padilla, H., Vergara, M., 1989. Low-grade regional metamorphism, in the Mesozoic-Cenozoic volcanic sequences of the Central Andes. J. Metamorph. Geol. 7, 487–495.

Liou, J.G., de Capitani, C., Frey, M., 1991. Zeolite equilibria in the system $CaAl_2Si_2O_8$–$NaAlSi_3O_8$–SiO_2–H_2O. N. Z. J. Geol. Geophys. 34, 293–301.

Merlet, C., 1994. An accurate computer correction program for quantitative electron probe micro-analysis. Mikrochim. Acta 114/115, 363–376.

Miron, G.D., Neuhoff, P.S., Amthauer, G., 2012. Low-temperature hydrothermal metamorphic mineralization of island-arc volcanics, South Apuseni Mountains, Romania. Clay Clay Miner. 60, 1–17.

Nawrocki, J., Panczyk, M., Williams, I.S., 2010. Isopotic ages and palaeomagnetism of selected magmatic rocks from King George Island (Antarctic Peninsula). J. Geol. Soc. 167 (5), 1063.

Neuhoff, P.S., Fridriksson, T., Arnorsson, S., 1999. Porosity evolution and mineral paragenesis during low-grade metamorphism of basaltic lavas at Teigarhorn, Eastern Iceland. Am. J. Sci. 299, 467–501.

Pallàs, R., Soriano, C., Zheng, X., Sabat, F., Casas, J.M., 1999. Volcanic Stratigraphy of Hannah Point, Livingston Island, South Shetland Islands, Antarctica. Acta Geol. Hisp. 34 (4), 323–328.

Palmason, G., Arnosson, S., Fridleifsson, I.B., 1979. The Iceland crust: evidence from drillhole data on structure and process. In: Talwani, M., Harrison, C.G.A., Hayes, D.E. (Eds.), Deep Drilling in the Atlantic Ocean, Ocean Crust. American Geophysical Union, Washington, D.C., pp. 43–65.

Pankhurst, R.J., Smellie, J.L., 1983. K-Ar geochronology of the South Shetland Islands, Lesser Antarctica: apparent lateral migration of Jurassic to Quaternary island arc volcanism. Earth Planet. Sci. Lett. 66, 214–222.

Robinson, D., Bevins, R.E., 1999. Patterns of regional low-grade metamorphism in metabasites. In: Frey, M., Robinson, D. (Eds.), Low-grade Metamorphism. Wiley-Blackwell, Ltd., London pp, pp. 143–168 (Chapter 3).

Schmidt, S.T., 1993. Regional and local patterns of low-grade metamorphism in the North Shore Volcanic Group, Minnesota, USA. J. Metamorph. Geol. 11, 401–414.

Smellie, J.L., 1979. The geology of Low Island, South Shetland Islands, and Austin rocks. Br. Antarct. Surv. 49, 239–257.
Smellie, J.L., Pankhurst, R.J., Thomson, M.R., Davies, R.E., 1984. The geology of the South Shetland Island: IV. Stratigraphy, geochemistry and evolution. Br. Antarct. Surv. 87 (85 pp.).
Smellie, J.L., Pallas, R., Sabat, F., Zheng, X., 1996. Age and correlation of volcanism in central Livingston Island, South Shetland Islands: K-Ar and geochemical constraints. J. S. Am. Earth Sci. 9, 265–272.
Solari, M., Hervé, F., Martinod, J., Le Roux, J., Ramírez, L., Palacios, C., 2008. Geotectonic evolution of the Bransfield Basin, Antarctic Peninsula: insights from analogue models. Antarct. Sci. 20 (02), 185–196.
Weisenberger, T., Selbekk, R.S., 2008. Multi-stage zeolite facies mineralization in the Hvalfjördur area, Iceland. Int. J. Earth Sci. http://dx.doi.org/10.1007/s00531-007-0296-6.
Willan, R., Armstrong, D., 2002. Successive hydrothermal, volcanic-hydrothermal and contact-metasomatic events in Cenozoic volcanic-arc basalts, South Shetland Islands, Antarctica. Geol. Mag. 132 (2), 209–231.
Willan, R., Kelley, S., 1999. Mafic dike swarms in the South Shetland Islands volcanic arc: unravelling multiepisodic magmatism related to subduction and continental rifting. J. Geophys. Res. 104, 23051–23068.